J. Fluid Mech. (2004), *vol.* 509, *pp.* 103–124.
DOI: 10.1017/S0022112004009061 Printed in the United Kingdom

On a new surfactant-driven fingering phenomenon in a Hele-Shaw cell

By R. KRECHETNIKOV AND G. M. HOMSY

University of California, Santa Barbara, CA 93106, USA

(Received 9 April 2003 and in revised form 12 January 2004)

According to the Saffman–Taylor criterion there is no instability when a more viscous fluid is displacing a less viscous one in a Hele-Shaw cell. Yet an instability was observed experimentally (Chan *et al.* 1997) in the same classical set-up but with the inner walls of the cell coated with surfactant solution. Linear stability analysis is applied to reveal the basic mechanism of this new instability. Asymptotic theory for low capillary numbers allows us to predict the long-wave instability, along with the dependence of the critical parameters on the material properties of the surfactant.

1. Introduction

One of the simplest and best studied instabilities occurring at the interface between two liquid phases is the Saffman–Taylor problem (cf. Saffman & Taylor 1958; Chuoke, van Meurs & van der Poel 1959) in which a more viscous fluid (μ_1, ρ_1) is displaced by a less viscous one (μ_2, ρ_2) in a Hele-Shaw cell (cf. Hele-Shaw 1898). The net effect of the instability is the formation of a viscous fingering pattern. The small gap, $2d$, between the plates forming the Hele-Shaw cell makes the motion effectively two-dimensional and potential. Indeed, after averaging the velocity field of the full Navier–Stokes equations over the direction perpendicular to the fluid velocity, we arrive at the Darcy's law approximation (cf. Darcy 1856), which results in a Laplace equation for the pressure field p in each fluid. The simplicity of the approximate mathematical formulation has allowed a straightforward linear stability analysis (cf. Saffman & Taylor 1958; Chuoke *et al.* 1959), the basic conclusion of which is the instability to all wavenumbers k except for the large ones damped by surface tension, as demonstrated by the expression for the leading (most unstable) eigenvalue λ,

$$\frac{3}{d^2}(\mu_1+\mu_2)\lambda = k\left\{\frac{3V}{d^2}(\mu_1-\mu_2)+g(\rho_1-\rho_2)\right\}-k^3\sigma,$$

and for the small ones cut off by the cell width. Here, the notation is standard, with V the displacement speed, σ the surface tension, μ the viscosity and ρ the density. If the surface tension is zero, the cut-off of the short wavelengths disappears. In the case of identical or negligible viscosities, the phenomenon reduces to the Rayleigh–Taylor instability (cf. Rayleigh 1900; Taylor 1950), while in the absence of the gravitational field, $g=0$, the effect of density differences disappears. When both effects are present (viscosity and gravity) and oppose one another, there exists a critical speed V_c of the threshold of instability.

The essential influence of the surface tension σ on the instability raises a natural question as to the effect of variations of the surface tension. While this effect belongs to the general class of problems with Marangoni phenomena, which include the

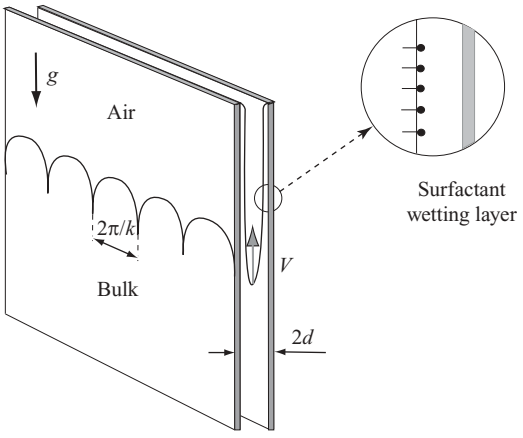

FIGURE 1. Fingering instability in a Hele-Shaw cell with pre-existing wetting layer of thickness $\bar{h}_\infty$.

variations of σ due to temperature gradients, electromagnetic field and surface active materials (surfactants), only the last subclass is studied in this paper. There are many examples of physical systems in which surfactants have a substantial effect on the fluid motion. One well-known effect refers back to experiments by Bond & Newton (1928), who found that the drag force experienced by small moving bubbles and drops is not in agreement with the Hadamard–Riabouchinsky formula for a clean interface drop, but is closer to that of a solid sphere. Two basic theories have been proposed to explain the phenomenon. Levich's theory (Levich 1948) refers to the case when the surfactant interfacial concentration remains almost constant and asymptotically small variations of the contaminant exert a retarding effect on the motion of the drop (bubble). On the other hand, the retarding mechanism in Savic's theory (Savic 1953) is due to surface convective formation of a stagnant cap, which is considered as a rigid film with a no-slip boundary condition, while the rest of the surface is covered by a mobile film with the usual dynamic condition. Levich's theory has been widely used in other problems and is a main tool of working with surface active substances, but is limited to trace amounts and asymptotically small gradients, as in works by Ratulowski & Chang (1900), Park (1992) and Waters & Grotberg (2002) to name a few. In our problem, we encounter the situation of large shear stresses, so that a Levich type analysis is not applicable. At the same time, we avoid using a discontinuous Savic theory, in view of the difficulty of treating surfactant concentration gradients crucial in our situation, but rather propose a mathematically consistent way of dealing with the physics of the phenomena while retaining the standard dynamic condition at the interface.

In the above example, like many others, surfactant-generated Marangoni effects just modify the existing solution to leading order, but do not introduce any new fundamental instabilities. The experiments conducted by Chan & Liang (1997), however, have demonstrated that surface-active substances crucially influence the Saffman–Taylor phenomenon and even reverse its stability characteristics. Figure 1 gives a diagram of the experiment: a Hele-Shaw cell is dipped into a surfactant solution at speed V. They observed instabilities when more viscous and more dense fluid displaces a less viscous and lighter one, under a specific condition – a pre-existing wetting layer of the surfactant solution inside the Hele-Shaw cell must be present, as shown in the insert in figure 1. Otherwise, the vertical motion of the cell

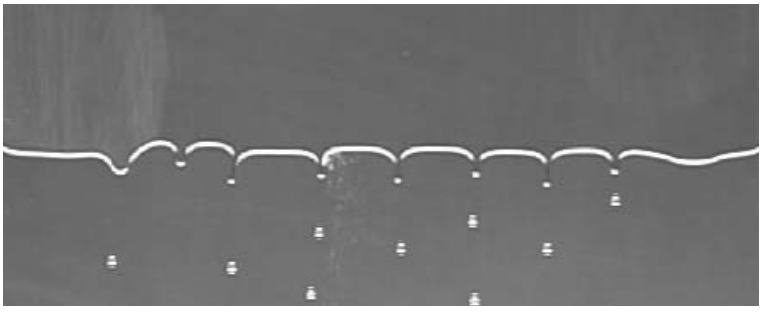

FIGURE 2. Fingering pattern of reversed Saffman–Taylor instability. The plates are moving into a surfactant solution, which is the lower phase in this photograph. A quasi-steady nonlinear wave pattern is observed.

produces no instability. Besides this crucial effect of the wetting layer, several other important observations and conclusions by Chan & Liang (1997) were made: (a) the formation of a long-wave steady-state pattern (above criticality, in a nonlinear regime, we observe fingers pointing in the direction opposite to motion with a well-defined characteristic length independent of system size); (b) the existence of a critical speed of dipping, when the instability is first observed, with dependence of its magnitude on the properties of the wetting layer; (c) the instability is observable below the critical micelle concentration (CMC). (However, Chan & Liang (1997) state that for clear and reproducable experiments they needed the solution to be above CMC); (d) an increase in concentration leads to a slight lowering of the critical speed. Figure 2, produced in our laboratory by J. Fernandez in 2003, illustrates some of the features of the instability. A Hele-Shaw cell with gap width 300 μm is driven at a speed of $3.8\,\mathrm{cm\,s^{-1}}$ into a 4.0 mM solution of SDS (CMC is about 8.2 mM). A regular pattern of steady standing waves of wavelength $\simeq 1$ cm is observed. In this case, the critical speed is approximately $0.51\,\mathrm{cm\,s^{-1}}$ and the waves are long compared to the characteristic gap dimension. In addition, experiments in our laboratory, suggested by the theory developed below, of dipping the Hele-Shaw cell with pre-existing surfactant wetting layer into the bulk not containing surfactants (J. Fernandez, personal communication 2003) have demonstrated that the only necessary condition for the instability is the presence of surfactants in the wetting layer. *A priori*, it is clear that addition of surface tension variation to the Saffman–Taylor set-up allows for a new driving force (Marangoni stresses), which competes with the stabilizing viscosity stratification and thus leads to an instability.

Theoretical studies of this problem had been initiated even before the above mentioned experiments were performed. Guo, Hong & Kurtze (1992, 1995) was the first work devoted to the effects of surfactants on displacement instabilities. They predicted a finite-amplitude instability using a non-physical state equation for the surface tension – a linear dependence on the surface curvature. However, it is clear that σ must at a minimum be a function of the surface surfactant concentration. However, the fact that experimental results have always indicated complete stability of a flat interface when the less viscous fluid is displaced by the more viscous one, led them to the speculation that, in practice, the threshold amplitude is quite large. As pointed out by Chan (2000), who has carried out experiments to find those instabilities, the predictions of Guo *et al.* (1992, 1995) are not observable. Also, Chan (2000) has proposed a linear stability analysis for the problem by modifying the *ansatz*

of Guo *et al.* (1992, 1995) by replacing the linear local dependence of σ on curvature by a dependence on the deformation of the interface. Again, the deficiency of this model is a non-physical state equation for σ and the inability to explain the crucial role of the pre-existing wetting layer in producing the instability.

The primary objective of our work is to formulate and analyse a model of the instability that couples surfactant effects to the flow equations in a realistic and physically plausible fashion. As correctly noted by Chan (2000), the phenomenon belongs to the class of *surfactant driven instabilities*; however, the breadth of this class necessitates a more precise description. We should also distinguish the cases where the surfactant-driven Marangoni stresses are the only mechanism to produce fluid motion, like a fingering instability in the spreading of surface active material on a thin liquid film studied by Troian, Wu & Safran (1989*a*) and Matar & Troian (1997). Experimentally, this is achieved by depositing a droplet of a surfactant solution on the surface of a clean water film. Their analysis hinges on the only driving mechanism being Marangoni stresses with neglect of (i) the effects of external forces, such as gravity, (ii) effects of curvature generating capillary pressure, and (iii) surfactant exchange between bulk and interface. Those three features distinguish the problem considered in this paper in a fundamental way: it belongs to a different subclass of surfactant-driven instabilities, where in addition to the Marangoni stresses there is another mechanism – the flow advection due to the plate motion. Further, the pre-existing wetting layer guarantees a transition region with non-negligible curvature and thus capillary pressure; and the solubility of the surfactant provides the exchange with bulk, a process that competes with the accumulation of the surfactants in a cap region. Despite the fact that our problem has a non-trivial basic state entailing complicated transient behavior of the disturbances, and contains more physical effects as discussed above, it admits a very clear and concise theoretical and physical interpretation.

The outline of the paper is as follows. In § 2, the mathematical set-up is introduced, which corresponds to the dipping of the Hele-Shaw cell with a pre-existing surfactant wetting layer into a bulk liquid in the direction parallel to the gravitational field as in experiments. However, it must be noted that gravity affects only certain scalings. The experiments by Chan & Liang (1997) and additional experiments by Fernandez in 2003 in our laboratory have suggested that the phenomenon is due to the accumulation of the surfactant in the cap region, thus potentially leading to high gradients of surfactant concentration. Therefore, the theory must be able not only to explain the above observations (a)–(d), but also to account for surfactant concentration gradients of the order of unity which ultimately allow the support of large shear stresses at the interface. The last requirement has motivated us to extend in § 3 the standard low-capillary number theoretical approach of surfactant-driven flows to this regime, which involves new ideas on Marangoni boundary layers at the interface. In § 4.1, this approach is exploited in the formulation of the linear stability equations, while in § 4.2, the appropriate dispersion relation is analysed to predict instability as related in § 4.3 to the experimental set-up of Chan (2000).

2. Problem formulation

In view of its rectangular geometry, the problem is naturally considered in a Cartesian system of coordinates (refer to figure 3) designated either by tensorial x_i, $i = 1, 2, 3$ or by the usual assignment $x_1 \to x$, $x_2 \to y$, $x_3 \to z$. The same concerns velocity field notations: $v_1 \to u$, $v_2 \to v$, $v_3 \to w$. The first coordinate (velocity

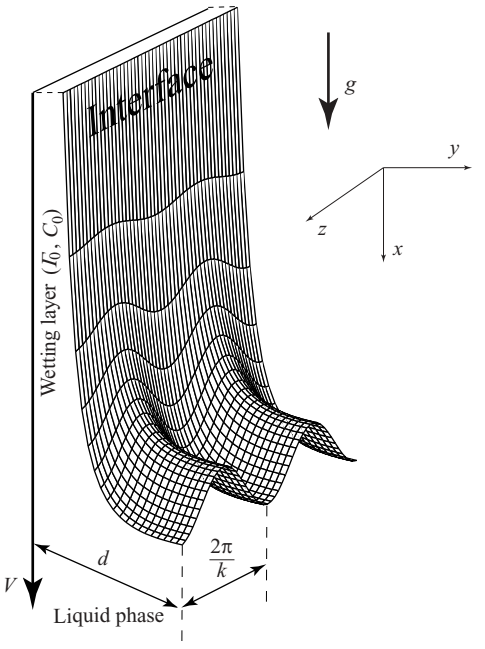

FIGURE 3. Theoretical set-up.

component) is directed downwards, the second is perpendicular to the cell plates and the third defines the direction in which the instability is sought. Since a liquid–gas interface is considered, we neglect the gas phase dynamics and formulate the equations for the liquid phase in the one-fluid approximation. The problem contains the following independent physical parameters: surfactant bulk and interfacial concentrations in the wetting layer C_0, Γ_0, two kinetic parameters (k_a, k_d rates of adsorption and desorption accordingly), surface diffusion coefficient D_s, two geometrical parameters (d half gap length, $\overline{h}_\infty$ pre-existing film thickness), the plate speed V, external field of gravity g, and three material properties of the liquid (ρ density, σ surface tension, μ dynamic viscosity).

All spatial coordinates are non-dimensiona-lized with respect to the half gap length d; the velocity field is scaled by the speed of the Hele-Shaw cell V; the characteristic time is defined accordingly as d/V. The surface and bulk surfactant concentrations are scaled with respect to the appropriate values in the pre-existing wetting layer, Γ_0 and C_0. The surface tension is non-dimensionalized by its value in the pre-existing wetting layer as well, $\sigma_0 = \sigma(\Gamma_0)$, and the pressure is scaled with respect to its capillary component σ_0/d. All substance properties are non-dimensionalized by the values in the liquid phase. According to the π-theorem the solution, eight dependent variables $(u, v, w, p, \gamma, C, h, \sigma)$ – depends on four independent variables (t, x, y, z), and eight non-dimensional parameters:

$$Ca = \frac{\mu V}{\sigma_0},\ Re = \frac{\rho V d}{\mu},\ Bo = \frac{d^2 \rho g}{\sigma_0},\ Pe_s = \frac{dV}{D_s},$$

$$St = \frac{k_a}{V}, K = \frac{k_a C_0}{k_d \Gamma_0},\ \kappa = \frac{dC_0}{\Gamma_0}\frac{1}{K}, h_\infty = \frac{\overline{h}_\infty}{d}.$$

Surface diffusion is actually much slower than the advection characteristic time; indeed, for the gap used in the experiments of Chan & Liang (1997), $d = 300\,\mu\text{m}$, $V \sim 1\,\text{cm}\,\text{s}^{-1}$ and estimating the surface diffusivity coefficient of the order of bulk diffusivity $10^{-10}\,\text{m}^{-2}\,\text{s}^{-1}$ (this assumption is within the range measured by Agrawal & Newman (1988), $(0.01 \div 7)10^{-9}\,\text{m}^{-2}\,\text{s}^{-1}$, cf. also Shen *et al.* (2002)), the Péclet number Pe_s associated with this process is considerably greater than unity. However, we do not neglect this physical process so that we can provide a more complete physical picture. Further, since we do not consider the bulk concentration dynamics, the Stanton number St and κ appear only as a product, but are kept separate here to highlight the Stanton number dependence. In our case the Reynolds number $Re \sim O(1)$; however, while it is clear that we need to apply the full Navier–Stokes equations in the whole region, we will be working only in a transition region, the characteristic thickness of which, as will be shown, is much less than that of the gap, so that the associated $Re \ll 1$. Since, in a low-Reynolds-number regime, we can neglect the nonlinear convection terms, the continuity and momentum equations of the liquid phase are given by

$$\begin{aligned} \frac{\partial u}{\partial x} + \frac{\partial v}{\partial y} + \frac{\partial w}{\partial z} &= 0, \\ Re\,Ca\frac{\partial u}{\partial t} - Bo + \frac{\partial p}{\partial x} &= Ca\,\Delta u, \\ Re\,Ca\frac{\partial v}{\partial t} + \frac{\partial p}{\partial y} &= Ca\,\Delta v, \\ Re\,Ca\frac{\partial w}{\partial t} + \frac{\partial p}{\partial z} &= Ca\,\Delta w. \end{aligned}$$

The above equations are subject to the no-slip boundary conditions at the wall:

$$y = -1 : u = 1,\ v = 0;$$

and the solution profiles at infinities:

$$\begin{aligned} &x = -\infty : u = 1,\ v = 0; \\ &x = +\infty : u = 1 + \tfrac{3}{2}(1 - h_\infty)(y^2 - 1),\ v = 0. \end{aligned}$$

The conditions at the interface:

$$F(t, x, y, z) = y \pm h(t, x, z) = 0, \tag{2.1}$$

read as (cf. Landau & Lifshitz 1987)

$$\text{kinematic:} \quad \boldsymbol{n}\cdot\boldsymbol{v} = -\frac{F_t}{|\nabla F|},$$

$$\text{dynamic:} \quad \left[p + \sigma\left(\frac{1}{r_1} + \frac{1}{r_2}\right)\right] n_i = Ca\ \tau_{ik} n_k - (\nabla_s \sigma \cdot \boldsymbol{I}_s)_i\,,$$

where $\boldsymbol{n}$ is the unit normal vector pointing into air phase 1, $\boldsymbol{I}_s = \boldsymbol{I} - \boldsymbol{nn}$ is an idemfactor (surface-unit tensor), $\nabla_s = \nabla - \nabla_{\boldsymbol{n}} = \boldsymbol{I}_s \nabla$ is a surface gradient operator, and $\tau_{ik} = \partial_i u_k + \partial_k u_i$ is the rate of strain tensor. The dynamics of interfacial surfactant concentration is governed by

$$\frac{\partial \gamma}{\partial t} + \nabla_s \cdot \left(\gamma \boldsymbol{v} - \frac{1}{Pe_s}\nabla_s \gamma\right) + \gamma(\nabla_s \cdot \boldsymbol{n})(\boldsymbol{v}\cdot\boldsymbol{n}) = -\frac{1}{Pe}\boldsymbol{n}\nabla C, \tag{2.2}$$

where $\boldsymbol{v} = I_s \boldsymbol{v}$ is an interfacial velocity. The solution of (2.2) is subject to the condition of boundedness and constant concentration Γ_0 in the pre-existing wetting layer. The last term in (2.2), which is the net flux of surfactant into the surface from the bulk phase, is modelled here by Langmuir sorption kinetics:

$$-\frac{1}{Pe}\boldsymbol{n}\nabla C = \kappa St[KC(1-\beta\gamma)-\gamma] \text{ with } \beta = \frac{\Gamma_0}{\Gamma_m}, \tag{2.3}$$

which is the principal mode of the surfactant transport (justified by the large value of the Péclet number and the separation of the corresponding diffusion and sorption time scales), so that surfactant interchange between surface and bulk is kinetically controlled. In (2.3), the first term governs adsorption, and the last negative term is responsible for desorption. In the static case and without surface diffusion, (2.2) reduces to the usual non-equilibrium Langmuir–Hinshelwood kinetics. With this approach, the bulk concentration C is kept fixed (in non-dimensional variables $C = 1$), so that the corresponding equation for C drops out of the analysis. The state equation $\sigma = \sigma(\Gamma)$, which is in general nonlinear, completes the problem formulation. We assume regular behavior of σ such that $\sigma_{max} = \sigma(0)$, $\sigma_{min} = \sigma(\Gamma_m)$ and $\sigma_\gamma \leqslant 0$ as follows from thermodynamic considerations (cf. Landau & Lifshitz 1980), where Γ_m is a saturation concentration.

The subsequent analysis will be considered on the branch $y = -h(t, x, z)$ of the interface (2.1), that is for $y \leqslant 0$ with $h \geqslant 0$, as shown in figure 3. In view of the non-flat geometry of the interface, we need some basic representations from the geometry on surfaces. The normal and tangent vectors to the interface are given by

$$\boldsymbol{n} = \frac{\nabla F}{|\nabla F|} = \frac{\boldsymbol{i}h_x + \boldsymbol{j} + \boldsymbol{k}h_z}{\sqrt{1+h_x^2+h_z^2}}, \boldsymbol{t}_1 = \frac{\boldsymbol{i} - \boldsymbol{j}h_x}{\sqrt{1+h_x^2+h_z^2}}, \boldsymbol{t}_2 = \frac{-\boldsymbol{j}h_z + \boldsymbol{k}}{\sqrt{1+h_x^2+h_z^2}}.$$

The surface gradient ∇_s is found to have the form:

$$\nabla_s = \nabla - \boldsymbol{n}(\boldsymbol{n}\cdot\nabla) = \boldsymbol{i}\frac{(1+h_z^2)\frac{\partial}{\partial x} - h_x\frac{\partial}{\partial y} - h_x h_z\frac{\partial}{\partial z}}{(1+h_x^2+h_z^2)} + \boldsymbol{j}\frac{-h_x\frac{\partial}{\partial x} + (h_x^2+h_z^2)\frac{\partial}{\partial y} - h_z\frac{\partial}{\partial z}}{(1+h_x^2+h_z^2)} + \boldsymbol{k}\frac{-h_x h_z\frac{\partial}{\partial x} - h_z\frac{\partial}{\partial y} + (1+h_x^2)\frac{\partial}{\partial z}}{(1+h_x^2+h_z^2)},$$

and interfacial velocity:

$$\boldsymbol{v} = \boldsymbol{i}\frac{(1+h_z^2)u - h_x v - h_x h_z w}{(1+h_x^2+h_z^2)} + \boldsymbol{j}\frac{-h_x u + (h_x^2+h_z^2)v - h_z w}{(1+h_x^2+h_z^2)} + \boldsymbol{k}\frac{-h_x h_z u - h_z v + (1+h_x^2)w}{(1+h_x^2+h_z^2)}.$$

Therefore, the kinematic condition becomes

$$\frac{\partial h}{\partial t} + u\frac{\partial h}{\partial x} + v + w\frac{\partial h}{\partial z} = 0,$$

while the dynamic condition can be decomposed into normal and tangential components:

$$\left[p+\sigma\left(\frac{1}{r_1}+\frac{1}{r_2}\right)\right]n_i^2 = Ca\ \tau_{ik}n_k n_i,$$
$$0 = Ca\ \tau_{ik}n_k t_i^{(1,2)} - (\nabla_s\sigma\cdot\boldsymbol{I}_s)_i\, t_i^{(1,2)},$$

or explicitly

$$p+\sigma\left(\frac{1}{r_1}+\frac{1}{r_2}\right) = 2\ Ca\frac{u_x h_x^2 + v_y + w_z h_z^2 + (u_y+v_x)h_x + (u_z+w_x)h_x h_z + (v_z+w_y)h_z}{1+h_x^2+h_z^2},$$
$$\partial_x\sigma - h_x\partial_y\sigma = Ca\frac{2(u_x-v_y)h_x + (u_y+v_x)\left(1-h_x^2\right) + s(u_z+w_x)h_z - (v_z+w_y)h_x h_z}{\sqrt{1+h_x^2+h_z^2}},$$
$$\partial_z\sigma - h_z\partial_y\sigma = Ca\frac{-2(v_y-w_z)h_z - (u_y+v_x)h_x h_z + (u_z+w_x)h_x + (v_z+w_y)\left(1-h_z^2\right)}{\sqrt{1+h_x^2+h_z^2}}.$$

The mean curvature for a general $h(t,x,z)$ is:

$$\tfrac{1}{2}\left(\frac{1}{r_1}+\frac{1}{r_2}\right) = -\tfrac{1}{2}\nabla_s\cdot\boldsymbol{n} = -\frac{h_{xx}\left(1+h_z^2\right) - 2h_x h_z h_{xz} + h_{zz}\left(1+h_x^2\right)}{2\left(1+h_x^2+h_z^2\right)^{3/2}}.$$

3. Basic state

Since the instability occurs in the z-direction, it is natural to consider translationally invariant two-dimensional basic states comprising steady solutions of the governing equations. Also, the analysis is confined to the *mobile* interface case; however, the generalization to the case when a rigid film appears in a cap region is straightforward. Even though for stability analysis we need just the asymptotics of the basic state solution for $-x \gg 1$, we give a complete discussion of the base state in order to introduce the important elements of the regime in which linear disturbances are evolved. To distinguish the solution for the basic state, we use capitals for dependent variables.

First of all, we must introduce the appropriate scaling for the problem and the reference point for that is the thickness of the pre-existing film. In general, this thickness will depend on the method by which it is created; here, we restrict ourselves to the case of dip coating since it was used in all experimental studies of the phenomena (cf. Chan & Liang 1997; Fernandez). In the case of low capillary number and negligible effect of inertia, the deposited film thickness is given by

$$\overline{h}_\infty \sim d\frac{Ca_d^{2/3}}{(Bo+\text{const})^{1/2}} \equiv d\,Ca_*^{2/3}, \quad Ca_d = \frac{\mu V_d}{\sigma}, \tag{3.1}$$

where the quantity Ca_* is introduced for convenience. In the absence of gravity or when the film is deposited on a horizontal surface by a moving semi-infinite bubble (cf. Bretherton 1961) or a plug (cf. Waters & Grotberg 2002) in a channel, the thickness is expressed as

$$\overline{h}_\infty \sim d\,Ca_d^{2/3}.$$

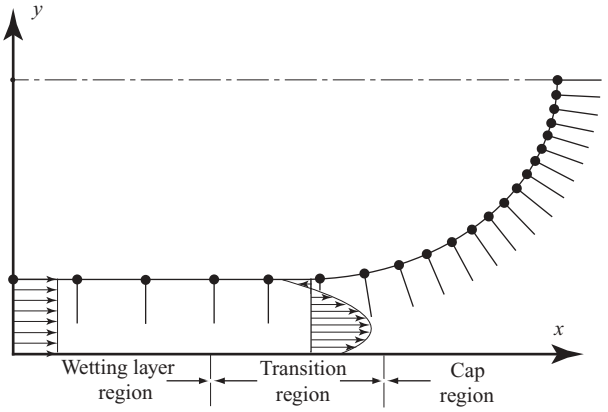

FIGURE 4. Division into regions.

On the other hand, if gravity dominates, the appropriate scale is the capillary length, $(\sigma/\rho g)^{1/2}$, and we have

$$\overline{h}_\infty \sim \left(\frac{\sigma}{\rho g}\right)^{1/2} Ca_d^{2/3},$$

(as originally obtained by Landau & Levich 1942) or rewritten in our non-dimensional variables:

$$\overline{h}_\infty \sim d\frac{Ca_d^{2/3}}{Bo^{1/2}}. \tag{3.2}$$

Here, the subscript d refers to the parameters of dip coating, since, in general, the speed V_d used to create the wetting film and that of dipping of the plate need not be the same; however, $Ca_* \sim Ca$ is assumed throughout our analysis. As follows from the above scaling, the analysis here is given for a vertical case at finite Bond number (as in Chan & Liang 1997), but clearly, gravity does not play any substantial role in the instability mechanism and reveals itself only in the scaling. While we use the scaling (3.2) in view of the particular experimental set-up, we can create the pre-existing layer by other means, for example by drawing from a Plateau border, without any effect on the analysis below.

Since the capillary number in our case is $Ca \sim 10^{-3}$ and $Bo \sim 10^{-2}$ (for $d = 300$ μm), we are justified in developing a low-capillary-number theory in the thin-film approximation. Under condition $g(\overline{h}_\infty^2/\nu V) \ll 1$ (gravity effects play a negligible role) the basic state in a thin-film region (far from the meniscus, cf. figure 4) corresponds to a constant pressure, $P = 0$, and trivial velocity profile:

$$u = 1,\ v = 0;\ C = 1,\ \Gamma = 1. \tag{3.3}$$

The problem of dip coating in the presence of an insoluble surfactant of dilute concentrations was considered by Park (1991). The solution in the constant-thickness-film region is matched with one in a cap region (cf. figure 4) with the help of a transition region as in Bretherton (1961) and Park & Homsy (1984). The order of the thickness of a pre-existing thin film dictates the following scaling for the transverse coordinate and interface shape:

$$y = -1 + Ca_*^{2/3}\widehat{y}, \qquad H = 1 - Ca_*^{2/3}\widehat{H},$$

where Ca_* is defined in (3.1), so that $\widehat{y}$ and $\widehat{H}$ are new variables of the order of unity. Also, the boundary conditions (3.3) dictate

$$P = \widehat{P}, \quad \Psi = Ca_*^{2/3}\widehat{\Psi}.$$

The unknown scaling for the x-coordinate is determined from the fact that the pressure gradient, P_x, must participate in the dynamics (otherwise matching with the solution in a cap region is not possible) and the term Ψ_{yyy} must also be retained to satisfy the boundary conditions. Therefore,

$$x = -l + \frac{Ca_*^{4/3}}{Ca}\widehat{x},$$

which corresponds to a thin-layer approximation, and the location of the origin l is determined in the course of matching. The use of these scalings results in the specific form of momentum equations

$$\left\{\frac{\partial \widehat{P}}{\partial \widehat{x}} - \widehat{\Psi}_{\widehat{y}\widehat{y}\widehat{y}}\right\} = \frac{Ca^2}{Ca_*^{4/3}}\,\widehat{\Psi}_{\widehat{x}\widehat{x}\widehat{y}} + Bo\,\frac{Ca_*^{4/3}}{Ca}, \tag{3.4}$$

$$\frac{\partial \widehat{P}}{\partial \widehat{y}} = -\frac{Ca^2}{Ca_*^{4/3}}\{Ca^2\widehat{\Psi}_{\widehat{x}\widehat{x}\widehat{x}} + \widehat{\Psi}_{\widehat{x}\widehat{y}\widehat{y}}\}.$$

The kinematic condition remains unchanged

$$\widehat{\Psi}_{\widehat{x}} + \widehat{H}_{\widehat{x}}\widehat{\Psi}_{\widehat{y}} = 0,$$

while the dynamic conditions become, to leading order,

$$\widehat{P} - \left(\frac{Ca}{Ca_*}\right)^2 \Sigma\,\widehat{H}_{\widehat{x}\widehat{x}} = -2\frac{Ca^2}{Ca_*^{4/3}}\{\widehat{\Psi}_{\widehat{x}\widehat{y}} + \widehat{H}_{\widehat{x}}\widehat{\Psi}_{\widehat{y}\widehat{y}}\}, \tag{3.5a}$$

$$\Sigma_{\widehat{x}} \equiv \frac{\mathrm{d}\Sigma}{\mathrm{d}\Gamma}(\Gamma)\frac{\mathrm{d}\Gamma}{\mathrm{d}\widehat{x}} = Ca_*^{2/3}\widehat{\Psi}_{\widehat{y}\widehat{y}}. \tag{3.5b}$$

The tangential condition indicates a strong nonlinear coupling with the surfactant dynamics:

$$\left(\partial_{\widehat{x}} + H_{\widehat{x}}\partial_{\widehat{y}}\right)(\Gamma \boldsymbol{v}) = \frac{Ca}{Ca_*^{4/3}}\frac{1}{Pe_s}\partial_{\widehat{x}}^2\Gamma + \frac{Ca_*^{4/3}}{Ca}\kappa St\,[KC(1-\beta\Gamma) - \Gamma],$$

where the variation in surfactant concentration resulting from the local changes in interfacial area is neglected as being higher order in $Ca_*^{2/3}(Ca/Ca_*)^2$. From the condition (3.5b) it follows that there are three possible consistent approximations, valid as $Ca \to 0$.

(i) The first is a Levich-type solution

$$\Gamma = \Gamma^* + Ca_*^{2/3}\widehat{\Gamma},\ \ \Gamma^* = \text{const} \Longrightarrow \Sigma_{\widehat{x}} = O\left(Ca_*^{2/3}\right),$$

which allows equilibration of the friction (shear stress) and Marangoni stress at the interface for small variations, $O(Ca_*^{2/3})$, of the surfactant concentration. In this limit, the Marangoni effect is moderate. We will call this scaling *the regular perturbation case*, which, as discussed in § 1, is widely used in the literature and corresponds to small gradients of surfactant concentration (cf. Ratulowski & Chang 1900; Park 1992;

Waters & Grotberg 2002). In this simple case, we immediately arrive at:

$$\widehat{P} - \left(\frac{Ca}{Ca_*}\right)^2 \Sigma(\Gamma^*)\widehat{H}_{\hat{x}\hat{x}} = O\left(Ca_*^{2/3}\ \left(\frac{Ca}{Ca_*}\right)^2\right), \tag{3.6a}$$

$$\frac{\mathrm{d}\Sigma}{\mathrm{d}\Gamma}(\Gamma^*)\frac{\mathrm{d}\widehat{\Gamma}}{\mathrm{d}\widehat{x}} = \widehat{\Psi}_{\hat{y}\hat{y}}, \tag{3.6b}$$

so that the dynamics of the flow field and interfacial surfactant concentration are coupled only through the tangential stress balance.

(ii) A second possibility is Savic's approach which allows us to accommodate significant variation of the surfactant concentration (cf. Savic 1953) and leads to a discontinuous solution $\Sigma_{\hat{x}}$ since (3.5*b*) is substituted by a no-slip boundary condition (see Davis & Acrivos 1966; Sadhal & Johnson 1983).

(iii) If the surfactant concentration changes in the main order over the scale of the transition region $\Sigma_{\hat{x}} \sim O(1)$, then the Marangoni effect is a dominating driving force. Indeed, $\Sigma_{\hat{x}} \sim O(1)$ implies $\widehat{\Psi}_{\hat{y}\hat{y}} \sim O(Ca_*^{-2/3})$ as demonstrated by the solution of (3.4) for the streamfunction

$$\widehat{\Psi} = \frac{\widehat{P}_{\hat{x}}}{6}\hat{y}^2(\hat{y} - 3\widehat{H}) + \frac{\hat{y}^2}{2}\frac{\Sigma_{\hat{x}}}{Ca_*^{2/3}} + \hat{y}, \tag{3.7}$$

since the x-component of the surface velocity

$$\widehat{u}_s = \widehat{\Psi}_{\hat{y}}|_{\hat{y}=\widehat{H}} = \frac{1}{Ca_*^{2/3}}\widetilde{u}_s^{(1)} + \widetilde{u}_s^{(2)} = \frac{1}{Ca_*^{2/3}}\left\{\Sigma_{\hat{x}}\widehat{H} + Ca_*^{2/3}\left(1 - \widehat{P}_{\hat{x}}\frac{\widehat{H}^2}{2}\right)\right\}, \tag{3.8}$$

where $\widetilde{u}_s^{(1,2)} \sim O(1)$. The singular character of this case is apparent from the presence of an inner scale

$$\hat{y} = \widehat{H} - Ca_*^{1/3}\widetilde{y},$$

governing the dynamics near the interface and which guarantees the equilibration of the shear and significant Marangoni stresses through the leading-order equations,

$$\widehat{P} + \left(\frac{Ca}{Ca_*}\right)^2 \Sigma\widehat{H}_{\hat{x}\hat{x}} = -2\left(\frac{Ca}{Ca_*}\right)^2 \widehat{H}_{\hat{x}}\widehat{\Psi}_{\widetilde{y}\widetilde{y}} + O\left(\frac{Ca^2}{Ca_*^{5/3}}\right),$$

$$\frac{\mathrm{d}\Sigma}{\mathrm{d}\Gamma}(\Gamma)\frac{\mathrm{d}\Gamma}{\mathrm{d}\hat{x}} = \widehat{\Psi}_{\widetilde{y}\widetilde{y}} + O(Ca_*),$$

$$\widehat{\Psi}_{\widetilde{y}\widetilde{y}\widetilde{y}} = O(Ca).$$

The flow in this sublayer is driven by the Marangoni stresses only and the capillary pressure is determined not only by curvature, but also by the normal viscous stresses. The dilute scaling, $\Gamma \leqslant O(Ca_*^{2/3})$, apparently recovers the well-studied case (3.6). In view of the analogy of the above problem to boundary-layer theory, we name the above limit *the singular perturbation case*. The presence of an inner scale $\widetilde{y}$ near the interface (see figure 5) implies a very high shear rate ($|\widehat{\Psi}_{\hat{y}\hat{y}}| \gg 1$), but does not mean the existence of separate boundary-layer and outer solutions. Actually, the inner scale in a boundary condition affects the complete solution as we can see from the tangential stress at the other boundary (at the wall):

$$\widehat{\Psi}_{\hat{y}\hat{y}}|_{\hat{y}=0} = -P_{\hat{x}}\widehat{H} + \frac{\Sigma_{\hat{x}}}{Ca_*^{2/3}}.$$

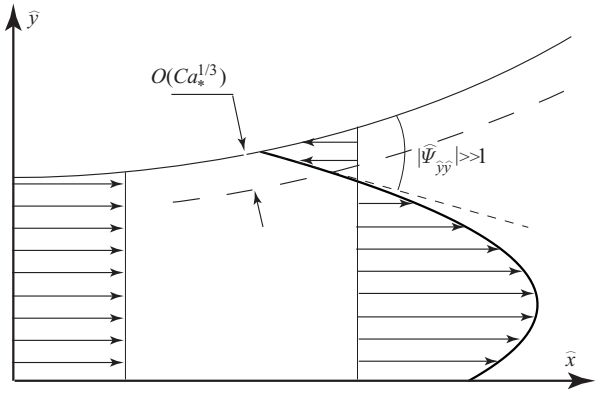

FIGURE 5. Boundary-layer structure in the transition region.

The presence of strong Marangoni stresses leads to motions in opposite directions near the interface and the wall, respectively. The pressure gradient adjusts itself through the normal and kinematic conditions so that the mass flux is conserved. The situation is analogous to the boundary-layer theory in aerodynamics, when the boundary layer of thickness $O(Re^{-1/2})$ is responsible for satisfying the no-slip condition at the wall versus the impermeability condition in the inviscid case, $Re=\infty$. In our case, the boundary layer of thickness $O(Ca_*^{1/3})$ allows us to satisfy a tangential component of the dynamic condition at the interface versus the no-stress condition in a zero-capillary-number case. As we can see, both limits – $Re\to\infty$ and $Ca\to 0$ – exhibit a singular behavior.

While the base state may be determined numerically from system (A 2)–(A 3) given in the Appendix, we find that since the instability is generated in the wetting layer, we do not need the complete solution, but only its asymptotics as $\hat{x}\to-\infty$. It is clear that the parallel approximation for the basic state is justified in this limit, since, in this regime, all basic state variables change on a slow scale. Indeed, the surface surfactant concentration should change from its maximum in the cap region $\Gamma_{max}\leqslant\Gamma_{sat}$ at $x=0$ to its value in the wetting layer, Γ_0 as $\hat{x}\to-\infty$, as indicated by boundary conditions for (A 3). The steady-state solution of (A 3) for $\hat{x}\to-\infty$ is of the trivial form $\Gamma=1$.

Summarizing, we stress that the study of the basic state in the transition region has led us to the appropriate theoretical framework corresponding to significant surface tension variation. The system (A 2)–(A 3) defines the solution for the basic state which matches with the one in the wetting-layer region and with another in the cap region. While, in general, its solution is complicated, the primary features can be seen from its general structure: Marangoni effects retard the interface motion so that surfactant is accumulated and increases in concentration. Intuitively, it is also clear that with the increase of speed of dipping, we should observe the increase of Γ for each fixed $\hat{x}$, until saturation is achieved owing to the effect of accumulation.

4. Evolution of infinitesimal disturbances

In this section, we demonstrate that the observed instability is an inherent property of a pre-existing wetting layer, which exhibits itself in this particular problem owing to accumulation of the surfactant in a cap region (cf. figure 4). Therefore, the peripheral effects, like non-parallelism, or $\hat{x}$-dependence, of the basic state can change the results

only quantitatively: the qualitative physics of the phenomenon can be understood from the asymptotic analysis of the parallel state.

4.1. *Linear disturbance equations*

The evolution of the complete field (basic state + disturbances) is considered on the same scales as the basic state:

$$t=\frac{Ca_*^{4/3}}{Ca}\,\hat{t},\quad x=-l+\frac{Ca_*^{4/3}}{Ca}\,\hat{x},\quad z=\frac{Ca_*^{4/3}}{Ca}\,\hat{z},$$
$$y=-1+Ca_*^{2/3}\hat{y},\quad h=1-Ca_*^{2/3}\hat{h},$$
$$p=\hat{p},\quad \psi=Ca_*^{2/3}\hat{\psi},\quad \varphi=Ca_*^{2/3}\hat{\varphi},$$

where the three-dimensional velocity field is represented by two streamfunctions $u=\psi_y$, $v=-\psi_x-\varphi_z$, $w=\varphi_y$ and the scales for z and φ are chosen from the principle of minimal degeneracy.

Because the basic state is known only with some degree of accuracy (in an asymptotic sense), the imposed disturbances are considered to have amplitudes much larger (again in asymptotic sense) than the truncated terms in the basic state solution expansion, but much less than unity (after appropriate rescaling). The complete flow field is governed by

$$\hat{u}_{\hat{x}}+\hat{v}_{\hat{y}}+\hat{w}_{\hat{z}}=0,$$
$$Re\,Ca\frac{\partial\hat{u}}{\partial\hat{t}}+\frac{\partial\hat{p}}{\partial\hat{x}}-Bo\,\frac{Ca_*^{4/3}}{Ca}=\frac{Ca^2}{Ca_*^{4/3}}(\hat{u}_{\hat{x}\hat{x}}+\hat{u}_{\hat{z}\hat{z}})+\hat{u}_{\hat{y}\hat{y}},$$
$$Re\,\frac{Ca^3}{Ca_*^{4/3}}\frac{\partial\hat{v}}{\partial\hat{t}}+\frac{\partial\hat{p}}{\partial\hat{y}}=\frac{Ca^4}{Ca_*^{4/3}}(\hat{v}_{\hat{x}\hat{x}}+\hat{v}_{\hat{z}\hat{z}})+\frac{Ca^2}{Ca_*^{4/3}}\hat{v}_{\hat{y}\hat{y}},$$
$$Re\,Ca\frac{\partial\hat{w}}{\partial\hat{t}}+\frac{\partial\hat{p}}{\partial\hat{z}}=\frac{Ca^2}{Ca_*^{4/3}}(\hat{w}_{\hat{x}\hat{x}}+\hat{w}_{\hat{z}\hat{z}})+\hat{w}_{\hat{y}\hat{y}},$$

and the kinematic condition can be written as

$$\frac{\partial\hat{h}}{\partial\hat{t}}+\hat{u}\frac{\partial\hat{h}}{\partial\hat{x}}-\hat{v}+\hat{w}\frac{\partial\hat{h}}{\partial\hat{z}}=0.$$

Further, we neglect the short-time-scale dynamics associated with the evolution of the velocity field. This is justified if we are interested in the leading-order eigenvalue only, but otherwise, for the construction of a complete spectrum, the accelerations cannot be neglected. The dynamic condition, after taking into account the leading-order terms, is of the form

$$\left.\begin{aligned}&\hat{p}+\left(\frac{Ca}{Ca_*}\right)^2\sigma(\hat{h}_{\hat{x}\hat{x}}+\hat{h}_{\hat{z}\hat{z}})=2\frac{Ca^2}{Ca_*^{4/3}}[\hat{v}_{\hat{y}}-\hat{u}_{\hat{y}}\hat{h}_{\hat{x}}-\hat{w}_{\hat{y}}\hat{h}_{\hat{z}}],\\&\partial_{\hat{x}}\sigma=Ca_*^{2/3}\hat{u}_{\hat{y}},\\&\partial_z\sigma=Ca_*^{2/3}\hat{w}_{\hat{y}},\end{aligned}\right\}\tag{4.1}$$

The dynamical system is closed by the equation for the evolution of interfacial surfactant concentration:

$$\partial_{\hat{t}}\hat{\gamma}+\partial_{\hat{x}}(\hat{\gamma}u_s)+\partial_{\hat{z}}(\hat{\gamma}w_s)=\frac{Ca}{Ca_*^{4/3}}\frac{1}{Pe_s}\left(\partial_{\hat{x}}^2+\partial_{\hat{z}}^2\right)\hat{\gamma}+\frac{Ca_*^{4/3}}{Ca}\kappa St\,[KC(1-\beta\hat{\gamma})-\hat{\gamma}],$$

and $C=1$ is assumed in the bulk phase. The above system, after decomposition into parallel basic state and disturbance fields,

$$\widehat{p}=\widehat{P}+\widehat{p}', \quad \widehat{\psi}=\widehat{\Psi}+\widehat{\psi}', \quad \widehat{\varphi}=\widehat{\Phi}(\equiv 0)+\widehat{\varphi}', \quad \widehat{\gamma}=\widehat{\Gamma}+\widehat{\gamma}', \quad \widehat{h}=\widehat{H}+\widehat{h}',$$

and linearization around the base state interface H, yields the leading-rder momentum equations for the disturbance in a quasi-steady approximation:

$$\left.\begin{aligned}
&\frac{\partial \widehat{p}'}{\partial \widehat{x}}=\widehat{\psi}'_{\widehat{y}\widehat{y}\widehat{y}},\\
&\frac{\partial \widehat{p}'}{\partial \widehat{y}}=0,\\
&\frac{\partial \widehat{p}'}{\partial \widehat{z}}=\widehat{\varphi}'_{\widehat{y}\widehat{y}\widehat{y}},\\
&\widehat{y}=0:\ \widehat{\psi}'_{\widehat{y}}=\widehat{\psi}'=\widehat{\varphi}'_{\widehat{y}}=\widehat{\varphi}'=0,
\end{aligned}\right\} \tag{4.2}$$

where the other boundary conditions come from the tangential components of the dynamic condition at the interface,

$$\left.\begin{aligned}
&\widehat{p}'+\left(\frac{Ca}{Ca_*}\right)^2 \Sigma\Delta\widehat{h}'=-2\left(\frac{Ca}{Ca_*}\right)^2 Ca_*^{2/3}[\widehat{\psi}'_{\widehat{x}\widehat{y}}+\widehat{\varphi}'_{\widehat{y}\widehat{z}}],\\
&\Sigma_\Gamma\widehat{\gamma}'_{\widehat{x}}=Ca_*^{2/3}\widehat{\psi}'_{\widehat{y}\widehat{y}},\\
&\Sigma_\Gamma\widehat{\gamma}'_{\widehat{z}}=Ca_*^{2/3}\widehat{\varphi}'_{\widehat{y}\widehat{z}},
\end{aligned}\right\} \tag{4.3}$$

and from the linearized kinematic condition

$$\widehat{h}'_{\widehat{t}}+\widehat{\Psi}_{\widehat{y}}\widehat{h}'_{\widehat{x}}+\widehat{\psi}'_{\widehat{x}}+\widehat{\varphi}'_{\widehat{z}}=0.$$

The governing system is closed by the equation for the evolution of interfacial surfactant concentration

$$\widehat{\gamma}'_{\widehat{t}}+\widehat{\Gamma}(\widehat{\psi}'_{\widehat{x}\widehat{y}}+\widehat{\varphi}'_{\widehat{y}\widehat{z}})+\widehat{\Psi}_{\widehat{y}}\widehat{\gamma}'_{\widehat{x}}=\frac{Ca}{Ca_*^{4/3}}\frac{1}{Pe_s}\Delta\widehat{\gamma}'-\frac{Ca_*^{4/3}}{Ca}\kappa St\,[K\beta+1]\,\widehat{\gamma}',$$

with the requirement of boundedness of $\widehat{\gamma}'$. After elimination of the velocity field, this system is simplified to

$$\left.\begin{aligned}
&\widehat{p}'=-\left(\frac{Ca}{Ca_*}\right)^2[\Sigma\Delta\widehat{h}'+2H\Sigma_\Gamma\Delta\widehat{\gamma}'],\\
&\widehat{\gamma}'_{\widehat{t}}+\widehat{\gamma}'_{\widehat{x}}=\widehat{\Gamma}\left(\frac{H^2}{2}\Delta\widehat{p}'-\frac{H\Sigma_\Gamma}{Ca_*^{2/3}}\Delta\widehat{\gamma}'\right)+\frac{Ca}{Ca_*^{4/3}}\frac{1}{Pe_s}\Delta\widehat{\gamma}'-\frac{Ca_*^{4/3}}{Ca}\kappa St[K\beta+1]\widehat{\gamma}',\\
&\widehat{h}'_{\widehat{t}}+\widehat{h}'_{\widehat{x}}=\frac{H^3}{3}\Delta\widehat{p}'-\frac{H^2}{2}\frac{\Sigma_\Gamma}{Ca_*^{2/3}}\Delta\widehat{\gamma}',
\end{aligned}\right\} \tag{4.4}$$

which, in the clean interface case, reduces to the one equation given by Troian *et al.* (1989*b*) in the parallel basic state limit. It is instructive to trace the physical origin/interpretation of the terms appearing in the system (4.4) as given in table 1.

$\widehat{h}'_{\hat{t}} + \widehat{h}'_{\hat{x}}$	Advection of the interface disturbance by the basic state flow field
$\widehat{\gamma}'_{\hat{t}} + \widehat{\gamma}'_{\hat{x}}$	Advection of the surfactant concentration disturbance by the basic state flow field
$\frac{H^3}{3}\Delta\widehat{p}'$	Advection of momentum due to the v (y-)component of the disturbance velocity field
$-\frac{H^2}{2}\frac{\Sigma_\Gamma}{Ca_*^{2/3}}\Delta\widehat{\gamma}'$	Advection of momentum due to the Marangoni stresses contribution into the v (y-)component of the disturbance velocity field
$-\widehat{\Gamma}\frac{H\Sigma_\Gamma}{Ca_*^{2/3}}\Delta\widehat{\gamma}'$	Advection of surfactant by the Marangoni-induced disturbance flow
$\frac{Ca}{Ca_*^{4/3}}\frac{1}{Pe_s}\Delta\widehat{\gamma}'$	Surface diffusion of surfactant
$-\frac{Ca_*^{4/3}}{Ca}\kappa St\,[K\beta+1]\,\widehat{\gamma}'$	Sorption–desorption kinetics of the disturbed surfactant concentration
$\widehat{\Gamma}\frac{H^2}{2}\Delta\widehat{p}'$	Advection of surfactant by pressure-driven perturbation flow
$-\left(\frac{Ca}{Ca_*}\right)^2\Sigma\Delta\widehat{h}'$	Capillary perturbation pressure due to surface deflection
$-2\left(\frac{Ca}{Ca_*}\right)^2 H\Sigma_\Gamma\Delta\widehat{\gamma}'$	Normal stress due to surfactant disturbances

TABLE 1. Physical interpretation of various terms in (4.4).

Further simplification of (4.4) amounts to elimination of the pressure field, which produces the coupled system

$$\left.\begin{aligned}\widehat{\gamma}'_{\hat{t}} + \widehat{\gamma}'_{\hat{x}} &= -\left[\widehat{\Gamma}\frac{H\Sigma_\Gamma}{Ca_*^{2/3}} - \frac{Ca}{Ca_*^{4/3}}\frac{1}{Pe_s}\right]\Delta\widehat{\gamma}' - \frac{Ca_*^{4/3}}{Ca}\kappa St[K\beta+1]\widehat{\gamma}' \\ &\quad - \frac{H^2}{2}\left(\frac{Ca}{Ca_*}\right)^2\Gamma\{\Sigma\Delta^2\widehat{h}' + 2H\Sigma_\Gamma\Delta^2\widehat{\gamma}'\}, \\ \widehat{h}'_{\hat{t}} + \widehat{h}'_{\hat{x}} &= -\frac{H^3}{3}\left(\frac{Ca}{Ca_*}\right)^2\{\Sigma\Delta^2\widehat{h}' + 2H\Sigma_\Gamma\Delta^2\widehat{\gamma}'\} - \frac{H^2}{2}\frac{\Sigma_\Gamma}{Ca_*^{2/3}}\Delta\widehat{\gamma}'.\end{aligned}\right\} \tag{4.5}$$

The terms involving the hyperdiffusion operator Δ^2 are interpreted physically as the capillary pressure gradients contributed by the curvature and Marangoni effects, while the regular diffusion operator Δ in the equation for $\widehat{h}'$ comes from the normal component of the disturbance velocity field driven by the Marangoni stresses. The analogous terms in the equation for $\widehat{\gamma}'$ are generated by the advection of the disturbance field driven by Marangoni stresses and by surface diffusion, respectively.

4.2. *Dispersion relation analysis*

System (4.5) is to be analysed to determine its dispersion relation for growth or decay of spanwise perturbations. Applying the transformations

$$\widehat{\gamma}' \to \Gamma\widetilde{\gamma}, \quad \widehat{h}' \to H\widetilde{h}; \quad (\widehat{x}, \widehat{z}) \to \xi(x, z), \quad \widehat{t} \to \tau t,$$

where

$$\tau = \frac{Ca}{Ca_*^{4/3}}\frac{1}{\kappa St[K\beta+1]}, \quad \xi^4 = \tau\frac{H^3}{3}\left(\frac{Ca}{Ca_*}\right)^2\Sigma(\Gamma),$$

yields the system for linear evolution of disturbances in the canonical form:

$$\widetilde{\gamma}'_{\tilde{t}} + a\widetilde{\gamma}'_{\tilde{x}} + \widetilde{\gamma} - (\zeta m + \eta)\,\Delta\widetilde{\gamma} = -\tfrac{3}{2}[\Delta^2\widetilde{h} - m\Delta^2\widetilde{\gamma}], \tag{4.6a}$$

$$\widetilde{h}'_{\tilde{t}} + a\widetilde{h}'_{\tilde{x}} = -[\Delta^2\widetilde{h} - m\Delta^2\widetilde{\gamma}] + \frac{\zeta m}{2}\Delta\widetilde{\gamma}. \tag{4.6b}$$

Here, we introduce:

$$m = -2\frac{\Gamma\Sigma_\Gamma}{\Sigma}, \quad \zeta = \frac{1}{2}\frac{1}{Ca_*^{1/3}}\left(\frac{3\Sigma}{H\kappa\, St\, Ca\,(K\beta+1)}\right)^{1/2}, \quad \eta = \frac{\tau}{\xi^2}\frac{Ca}{Ca_*^{4/3}}\frac{1}{Pe_s}, \quad a = \frac{\tau}{\xi}.$$

The parameter m is taken as the primary bifurcation parameter containing the physics of the surfactant material behavior, while ζ and η reflect the effects of sorption–desorption kinetics and surface-diffusion, respectively.

We can see from (4.6*a*) that the effects of surface tension (capillary pressure), surface diffusion and bulk-interface interchange ($St > 0$) are stabilizing, while the effect of the Marangoni stresses (recall that $\Sigma_\gamma < 0$) is destabilizing as it comes from the normal dynamical condition and the Marangoni effect originating from the advection of surfactant by the Marangoni-induced disturbance flow is stabilizing. As we will see from the normal mode analysis, the destabilizing Marangoni effect overcomes the stabilizing role of the other contributors and produces the complicated instability phenomenon. Assuming the normal mode of the disturbance to be of the form

$$\begin{pmatrix} \widetilde{\gamma} \\ \widetilde{h} \end{pmatrix} = \mathrm{e}^{\lambda\tilde{t}+ik\tilde{z}+\varepsilon\tilde{x}} \begin{pmatrix} \bar{\gamma} \\ \bar{h} \end{pmatrix}, \quad \mathrm{Re}(\varepsilon) > 0,$$

where ε stands for the rate of the disturbance decay as $\tilde{x} \to -\infty$ (which is, in general, determined from matching to the solution for the disturbance in the cap region), we find that the dispersion relation is a function of the scaled wavenumber k, the material behavior m, sorption–desorption kinetics ζ and the surface diffusion η:

$$\lambda^2 + b\lambda + c = 0, \tag{4.7}$$

with

$$b = 2a\varepsilon + 1 + \left(1 - \tfrac{3}{2}m\right)\delta^2 + (\zeta m + \eta)\delta,$$
$$c = (a\varepsilon + \delta^2)\left(1 + a\varepsilon + \delta(\zeta m + \eta) - \tfrac{3}{2}m\delta^2\right) - \tfrac{3}{2}m\delta^2\left(\tfrac{1}{2}\zeta\delta - \delta^2\right),$$

where $\delta = k^2 - \varepsilon^2$. As a limiting case, eigenvalue analysis for the clean interface case, $\Sigma_\gamma = 0$, yields, to the leading order (assuming small ε and η),

$$\lambda = -k^2 \leqslant 0,$$

while in the presence of surfactants, the largest growth rate corresponds to zero wavenumber (while in reality there is a cut-off due to finite cell width)

$$\lambda = -2(1 - m\varepsilon^2\zeta) + O(\varepsilon),$$

so that the critical bifurcation parameter corresponds to

$$m \sim \frac{1}{\zeta\varepsilon^2}. \tag{4.8}$$

This instability can be understood as the effect of thickening of the transition region owing to Marangoni stresses (cf. figure 5) – the growth of the v component of the disturbance velocity. In general, the eigenvalues are found from the dispersion relation

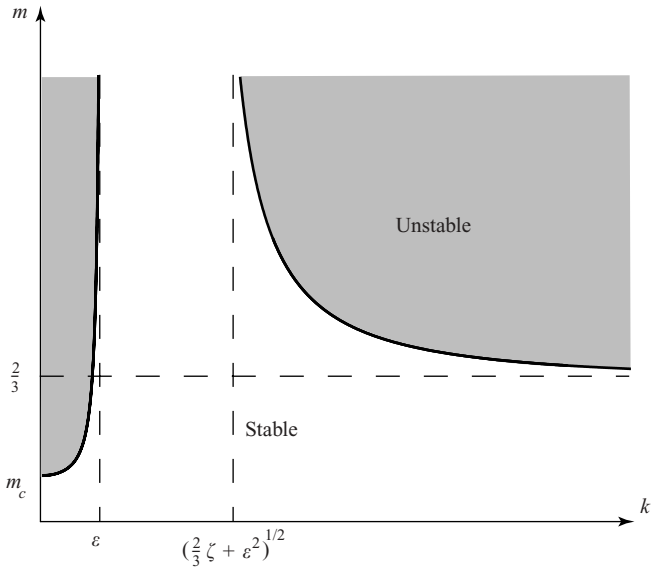

FIGURE 6. Locus of $\mathrm{Re}(\lambda_1)=0$. The bold curves correspond to the marginal stability conditions. The flow is unstable above and stable below these curves.

(4.7) with the appropriate eigenvectors

$$\begin{pmatrix} \widetilde{h} \\ \widetilde{\gamma} \end{pmatrix}_{1,2} = \begin{pmatrix} m - \dfrac{\lambda_{1,2} + a\varepsilon + 1 + (\zeta m + \eta)\delta}{\frac{3}{2}\delta^2} \\ 1 \end{pmatrix}.$$

Different branches of the marginal stability curve are defined by

$$b=0 \quad (c>0)\colon m = \frac{2a\varepsilon + 1 + \delta^2 + \eta\delta}{\frac{3}{2}\delta^2 - \zeta\delta},$$

so that, as $k^2 \to +\infty\colon m \to 2/3$, and by

$$c=0 \quad (b>0)\colon m = \frac{(a\varepsilon + \delta^2)(1 + a\varepsilon + \eta\delta)}{\frac{3}{2}a\varepsilon\delta^2 - \zeta\delta\left(a\varepsilon + \frac{1}{4}\delta^2\right)},$$

which gives the critical value (4.8) at zero wavenumber for small η and ε and large ζ (since $\zeta \sim Ca^{-1/2}Ca_*^{-1/3}$). It should be noticed that the following dependence for the bifurcation parameter

$$m \sim H^{1/2},$$

has non-trivial physical consequences, as will be discussed in a forthcoming publication. Thus, the global bifurcation point is given by

$$\left(k_c = 0, \quad m_c = \frac{1}{\zeta\varepsilon^2}\right).$$

The locus of $\mathrm{Re}(\lambda_1)=0$ for the most unstable eigenvalue λ_1 in the case $\zeta \gg 1$, $\varepsilon \ll 1$, $\eta \ll 1$ is depicted in figure 6 as a bold curve and essentially means that for any $m > m_c$ there exist wavenumbers k near the origin such that the instability takes place.

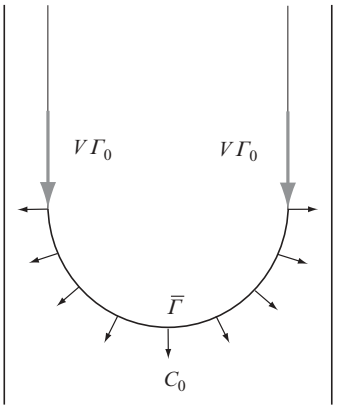

FIGURE 7. Surfactant transport in a cap region.

The functional form of the global bifurcation parameter indicates that $\Gamma_c \sim St^{1/2}$ as $St \to 0$ (when the surfactant becomes insoluble). However, absolute insolubility represents a singular limit – in this case the steady-state solution is a constant concentration in the cap and transition region, and a shock propagating with the dipping speed along the interface. In the case $St = 0$, the surface is uniformly covered by surfactant and no instability is expected since the inevitable monolayer collapse cannot produce significant macroscopic gradients in surface tension.

It should be mentioned that the instability found here is essentially a three-dimensional effect: the energy of the basic state/disturbance in the x-dimension is transferred to the z-dimension, in which the instability is observed. This differentiates this type of instability from the classical work by Sternling & Scriven (1959), where only two-dimensional disturbances were treated.

4.3. *Connection to experiments*

As we can see from (4.8), there is no dependence of the stability parameter on the speed of dipping since $Ca\,St$ is independent of V: the above analysis corresponds to the intrinsic instability of the interface, which is independent of its motion. Of course, a true free film does not exhibit instability in view of a homogeneous distribution of surfactant in a state of equilibrium. Thus, the instability appears only under conditions favourable to the creation of significant gradients in surfactant concentration. The problem considered here is one of those cases: the effect of the accumulation of surfactant in a cap region owing to the motion of the plates is the mechanism by which the required concentration gradients are produced at the interface.

In order to connect the intrinsic instability of a thin film with the effect of accumulation, we must use the appropriate expression for the surfactant concentration Γ. From a simple balance of surfactant transport in a cap region (cf. figure 7), we have

$$-2\Gamma_0 V = l[k_a C_0(1-\beta\Gamma) - k_d\Gamma_0\Gamma],$$

with l being the length of the meniscus, $l \simeq \pi d$, the effect of accumulation results in

$$\Gamma = \frac{1 + 2\dfrac{d}{l}\dfrac{1}{St\kappa'}}{\beta\left(1 + \dfrac{1}{\beta K}\right)} \text{ with } \kappa' = \frac{dC_0}{\Gamma_0}.$$

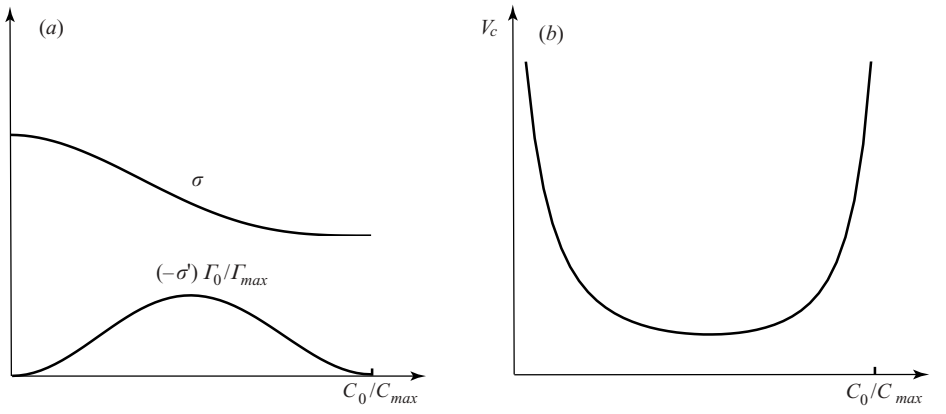

FIGURE 8. General features of RST instability. (*a*) Generic material behaviour of surfactants. (*b*) Qualitative dependence of critical speed on surface concentration, as inferred from (*a*) and equation (4.9).

This linear approximation does not account for either nonlinear or saturation phenomena, but nevertheless is valid for a wide range of speeds since $V \ll d\ k_d$ in most cases. Using this fact, (4.8) can be simplified to

$$v_c \equiv \frac{V_c}{lk_d} = \frac{1 + K_m\chi}{2}\left(A\frac{\sigma^{1/2}}{(-\sigma')}\frac{\widehat{H}^{1/2}}{\chi\,(1+K_m\chi)^{1/2}} - 1\right), \quad A = \left(\frac{Ca\ St\kappa}{3}\right)^{1/2}\frac{Ca_*^{1/3}}{\varepsilon^2}, \tag{4.9}$$

where $K_m = k_a C_m / k_d \Gamma_m$, σ is considered as a function of $C_0/C_m \equiv \chi$ and σ' is a derivative with respect to the argument. Further, using typical material behavior of pure surfactants $\sigma(\chi)$, as shown in figure 8(*a*), the critical speed ratio v_c as a function of the bulk concentration χ in a pre-existing wetting layer has the generic behavior shown in figure 8(*b*). The first asymptote corresponds to the limit $\chi \to 0$, while the second is associated with the saturation phenomena close to CMC. Notably, we predict no instability for $C > C_{CMC}$, in contrast to the claims in Chan & Liang (1997).

5. Conclusions

In this work, we have developed the elementary mathematical and physical interpretations for the experimentally observed instability. In particular, the crucial role of a pre-existing wetting layer of surfactant is revealed. In summary, the instability is due to the effect of the thickening of the wetting layer caused by significant Marangoni stresses, which, in turn, originate in the accumulation of surfactants in the cap and transition regions. As a necessary tool for developing the theory, we generalized the currently accepted one to the case of substantial surfactant concentration gradients.

While our analysis provides a robust explanation of the basic physical mechanism of the instability, a number of simplifications have been made. First of all, a simple mechanism for transport phenomena – kinetics-controlled bulk-surface exchange with fixed the kinetic constants – has been assumed. However, in reality, these constants may exhibit a strong dependence on concentration and thus on velocity as well. Accounting for these and other effects, e.g. the non-parallelism of the basic state

in the transition region, will lead to refinement of the theory and thus allow a quantitative comparison with experimental observations.

The authors would like to thank Dr Juan Fernandez for conducting experiments which allowed us to gain insight into this phenomenon and to verify the theoretical findings. This work was supported by the Office of Basic Energy Sciences, U S Department of Energy.

Appendix. Basic state equations

The equations governing the dynamics of the basic state are the solution for the stream function (3.7) and the normal component of the interface condition:

$$\widehat{P} = -\left(\frac{Ca}{Ca_*}\right)^2 \{\Sigma \widehat{H}_{\hat{x}\hat{x}} + 2(\widehat{H}\Sigma_{\hat{x}})_{\hat{x}}\}, \tag{A 1}$$

The condition $\Psi(\widehat{H}) = \widehat{H}_{-\infty}$ defines the equation for the interface shape with the following boundary conditions

$$\begin{aligned} &\hat{x} \to -\infty\colon \Gamma = C = \widehat{u}_s = 1,\ \ \widehat{H} = \widehat{H}_{-\infty};\\ &\hat{x} \to +\infty\colon \ \text{problem-dependent,} \end{aligned}$$

where the last condition is determined by matching with the solution in a cap region. From the condition $\widehat{\Psi}(\hat{y} = \widehat{H}) = \widehat{H}_{-\infty}$ using (3.7) and (A 1), we arrive at the following equation for the interface shape:

$$\left.\begin{aligned} &-\left(\frac{Ca}{Ca_*}\right)^2 \{\Sigma \widehat{H}_{\hat{x}\hat{x}} + 2(\widehat{H}\Sigma_{\hat{x}})_{\hat{x}}\}\frac{\widehat{H}^3}{3} = \frac{\widehat{H}^2}{2}\frac{\Sigma_{\hat{x}}}{Ca_*^{2/3}} + (\widehat{H} - \widehat{H}_{-\infty}),\\ &\hat{x} \to -\infty\colon \widehat{H} \to \widehat{H}_{-\infty},\ \widehat{H}_{\hat{x}} \to 0,\\ &\hat{x} \to +\infty\colon \ \widehat{H}_{\hat{x}\hat{x}} \to \sqrt{\frac{2}{\Sigma}}\frac{1}{Bo}. \end{aligned}\right\} \tag{A 2}$$

This system in the case $\Sigma = \text{constant}$ reduces to that derived in a seminal work by Landau & Levich (1942). The last boundary condition represents matching the curvature of the transition region interface to that of the meniscus region. For example, under the assumption of a uniform surfactant concentration in the cap region ($\Gamma = \Gamma^* = \text{const}$):

$$\lim_{\hat{x} \to +\infty} \{1 - Ca_*^{2/3}\ \widehat{H}\} = \lim_{x \to -l} H(x) = H(-l) + H_x(-l)(x + l) + H_{xx}(-l)\frac{(x + l)^2}{2} + \cdots.$$

Since a constant surface tension defines the simple shape of the cap

$$H(x) = \sqrt{\frac{\Sigma}{Bo}}\left\{\operatorname{sech}^{-1}\left(-\frac{x}{2}\sqrt{\frac{Bo}{\Sigma}}\right) - \sqrt{4 - \frac{Bo}{\Sigma}x^2}\right\} + \text{const},$$

we find $l = \sqrt{2\Sigma/Bo}$ and the appropriate matching of curvature.

Equation (A 2) is not closed until the surface tension variation is determined. This in turn is defined by the surfactant distribution which is governed by (surface diffusion

is neglected here being of the order of $Ca^{1/3}/Pe_s$)

$$\left.\begin{aligned} &\partial_{\hat{x}}(\Gamma \hat{u}_s) = \frac{Ca}{Ca_*^{4/3}} \frac{1}{Pe_s} \partial_{\hat{x}}^2 \Gamma + \frac{Ca_*^{4/3}}{Ca} \kappa St \left[KC(1-\beta\Gamma) - \Gamma\right], \\ &\hat{x} \to -\infty\colon \Gamma = 1, \\ &\hat{x} \to +\infty\colon \Gamma = \Gamma_{max}. \end{aligned}\right\} \tag{A 3}$$

Here, $\hat{u}_s$ is given by (3.8) and all terms must be retained to satisfy

$$\hat{x} \to -\infty\colon \hat{u}_s = 1.$$

The equation for the surface concentration indicates that advection is the primary mechanism controlling the surfactant distribution (the terms on the left-hand side of (A 3)), while the magnitude of Γ is determined by the kinetic exchange with the bulk (the second term on the right-hand side of (A 3)). The higher-order terms on the left-hand side of (A 3) are responsible for the advection of the surfactant due to the motion of plates and the capillary pressure gradient.

REFERENCES

Agrawal, M. L. & Newman, R. D. 1988 Surface diffusion in monomolecular films. II. Experiment and theory. *J. Colloid Interface Sci.* **121**, 366–380.

Bond, W. N. & Newton, D. A. 1928 Bubbles, drops, and particles. *Phil. Mag.* **5**, 794–800.

Bretherton, F. P. 1961 The motion of long bubbles in tubes. *J. Fluid Mech.* **10**, 166–188.

Chang, C.-H. & Franses, E. I. 1995 Adsorption dynamics of surfactants at the air/water interface: a critical review of methematical models, data, and mechanisms. *Colloids Surfaces* A **100**, 1–45.

Chan, C. K. 2000 Surfactant wetting layer driven instability in a Hele-Shaw cell. *Physica* A **288**, 315–325.

Chan, C. K. & Liang, N. Y. 1997 Observations of surfactant driven instability in a Hele-Shaw Cell. *Phys. Rev. Lett.* **79**, 4381–4384.

Chuoke, R. L., van Meurs, P. & van der Poel, C. 1959 The instability of slow, immiscible, viscous liquid–liquid displacements in permeable media. *Petrol. Trans. AIME* **216**, 188–194.

Darcy, H. 1856 *Les Fontaines Publiques de la Ville de Dijon.* Victor Dalmond.

Davis, R. E. & Acrivos, A. 1966 The influence of surfactants on the creeping motion of bubbles *Chem. Engng Sci.* **21**, 681–685.

Guo, H., Hong, D. C. & Kurtze, D. A. 1992 Surface-tension-driven nonlinear instability in viscous fingers. *Phys. Rev. Lett.* **69**, 1520–1523.

Guo, H., Hong, D. C. & Kurtze, D. A. 1995 Dynamics of viscous fingers and threshold instability. *Phys. Rev.* E **51**, 4469–4478.

Hele-Shaw, H. S. 1898 On the motion of a viscous fluid between two parallel plates. *Trans. R. Inst. Nav. Archit. Lond.* **40**, 218.

Landau, L. D. & Levich, V. G. 1942 Dragging of a liquid by a moving plate. *Acta Physicochim.* **17**, 42–54.

Landau, L. D. & Lifshitz, E. M. 1987 *Fluid Mechanics.* Pergamon.

Landau, L. D. & Lifshitz, E. M. 1980 *Statistical Physics.* Pergamon.

Levich, V. G. 1948 Diffusion kinetics theory of heterogeneous chemical processes. *Z. Fiz. Khim.* **22**, 721–729.

Matar, O. K. & Troian, S. M. 1997 Linear stability analysis of an insoluble surfactant monolayer spreading on a thin liquid film. *Phys. Fluids* **9**, 3645–3657.

Park, C.-W. 1991 Effects of insoluble surfactants on dip coating. *J. Colloid Interface Sci.* **146**, 383–394.

Park, C.-W. 1992 Influence of soluble surfactants on the motion of a finite bubble in a capillary tube. *Phys. Fluids* A **4**, 2335–2347.

Park, C.-W. & Homsy, G. M. 1984 Two-phase displacement in Hele-Shaw cells: theory. *J. Fluid Mech.* **139**, 291–308.

Ratulowski, J. & Chang, H.-C. 1990 Marangoni effects of trace impurities on the motion of long gas bubbles in capillaries. *J. Fluid Mech.* **210**, 303–328.

Rayleigh, Lord 1900 Investigation of the character of the equilibrium of an incompressible heavy fluid of variable density. *Scientific Papers, Vol. II*, pp. 200–207. Cambridge University Press.

Sadhal, S. S. & Johnson, R. E. 1983 Stokes flow past bubbles and drops partially coated with thin films. Part 1. Stagnant cap of a surfactant film – exact solution. *J. Fluid Mech.* **126**, 237–250.

Saffman, P. G. & Taylor, G. 1958 The penetration of a fluid into a porous medium or Hele-Shaw cell containing a more viscous liquid. *Proc. R. Soc. Lond.* A **245**, 312–329.

Savic, P. 1953 Circulation and distortion of liquid drops falling through a viscous medium. *Natl Res. Counc. Can., Div. Mech. Engng Rep. MT-22.*

Shen, A. Q., Gleason, B., McKinley, G. H. & Stone, H. A. 2002 Fiber coating with surfactant solutions. *Phys. Fluids* **14**, 4055–4068.

Sternling, C. V. & Scriven, L. E. 1959 Interfacial turbulence: hydrodynamic stability and the Marangoni effect. *AIChE J.* **5**, 514–523.

Taylor, G. I. 1950 The instability of liquid surfaces when accelerated in a direction perpendicular to their planes. *Proc. R. Soc. Lond.* A **201**, 192–196.

Troian, S. M., Herbolzheimer, E., Safran, S. A. & Joanny, J. F. 1989*b* Fingering instability in thin wetting films. *Europhys. Lett.* **10**, 25–30.

Troian, S. M., Wu, X. L. & Safran, S. A. 1989*a* Fingering instability in thin wetting films. *Phys. Rev. Lett.* **62**, 1496–1499.

Waters, S. L. & Grotberg, J. B. 2002 The propagation of a surfactant laden liquid plug in a capillary tube. *Phys. Fluids* **14**, 471–480.